

Phase separation *versus* supersolid behavior in frustrated antiferromagnets

A. Fabricio Albuquerque,^{1,2} Nicolas Laflorencie,³ Jean-David Picon,^{4,5} and Frédéric Mila⁵

¹Laboratoire de Physique Théorique, CNRS and Université de Toulouse, F-31062 Toulouse, France

²School of Physics, The University of New South Wales, Sydney, NSW 2052, Australia

³Laboratoire de Physique des Solides, Université Paris-Sud, UMR-8502 CNRS, 91405 Orsay, France

⁴Theoretische Physik, ETH Zürich, 8093 Zürich, Switzerland

⁵Institute of Theoretical Physics, École Polytechnique Fédérale de Lausanne, CH-1015 Lausanne, Switzerland

(Dated: October 4, 2018)

We investigate the competition between spin-supersolidity and phase separation in a frustrated spin-half model of weakly coupled dimers. We start by considering systems of hard-core bosons on the square lattice, onto which the low-energy physics of the herein investigated spin model can be mapped, and devise a criterion for gauging the interplay between supersolid order and domain wall formation based on strong coupling arguments. Effective bosonic models for the spin model are derived via the contractor renormalization (CORE) algorithm and we propose to combine a self-consistent cluster mean-field solution with our criterion for the occurrence of phase separation to derive the phase diagram as a function of frustration and magnetic field. In the limit of strong frustration, the model is shown to be unstable toward phase separation, in contradiction with recently published results. However, a region of stable supersolidity is identified for intermediate frustration, in a parameter range not investigated so far and of possible experimental relevance.

PACS numbers: 75.10.Jm, 03.75.Nt, 05.30.Jp

I. INTRODUCTION

Dimer-based antiferromagnets (DAFs) under a magnetic field are promising candidates for displaying new phases of bosonic matter.¹ Magnetic excitations in such systems, termed *triplons*, are well described by lattice models of interacting bosons, whose density can be finely tuned by varying the magnitude of the applied field.^{2,3} Experimentally, field-induced Bose-Einstein condensation (BEC) of triplons has been observed in a number of DAFs (see the review Ref. 1) and, remarkably, exotic quantum criticality has been detected in the spin-dimer compound BaCuSi₂O₆.⁴⁻⁷ The presence of magnetic frustration further adds to the rich phenomenology of these systems by enhancing repulsive interactions between triplons, something that may eventually stabilize incompressible phases that break the lattice's translational symmetry.^{2,8} Such *crystalline* phases are for instance realized in the Shastry-Sutherland material SrCu₂(BO₃)₂,^{9,10} where they are signaled by a series of magnetization plateaux at unconventional fillings stabilized by complex triplon interactions.¹¹

The occurrence of both BEC and solid phases in the phase diagram of DAFs under magnetic field suggests that the magnetic equivalent of the phase simultaneously displaying diagonal and off-diagonal order known as *supersolid* (SS)¹²⁻¹⁴ may be realized in these systems. Indeed, insofar as more exotic possibilities are excluded,¹⁵ according to the Ginzburg-Landau-Wilson paradigm a continuous transition between phases breaking different symmetries (as it is the case with BEC and crystalline phases) is precluded and we are therefore left with two possibilities: (i) a first-order transition or (ii) the appearance of an intermediate phase, where both order parameters coexist, termed spin-supersolid (spin-SS) in

the present context. The latter possibility has been first investigated by Momoi and Totsuka for the Shastry-Sutherland model in the vicinity of half- and third-filling plateaux,¹⁶ based on a mean-field analysis of an effective bosonic model derived up to third-order in the inter-dimer coupling. More recently,¹¹ state-of-the-art techniques have been employed in deriving effective models that improve upon the third-order effective Hamiltonian of Ref. 16. Unfortunately, the reliability of these methods is still limited to inter-dimer couplings equal to, at most, one-half of the intra-dimer coupling, and in that parameter range the different plateaux seem to be separated by first-order transitions without any convincing evidence of spin-SS phases.¹¹

The situation is much clearer for the DAF investigated in Ref. 17 where repulsion among triplons are enhanced due to the strong Ising-like character of the inter-dimer exchange [see Eq. (1) in Ref. 18], making room for checkerboard solid (CBS) and spin-SS phases to emerge. The absence of frustration allows for quantum Monte Carlo (QMC) simulations to be performed and, in this way, the occurrence of a spin-SS phase for the model studied in Ref. 17 has been firmly established. However, such a strongly anisotropic Hamiltonian is unrealistic for Mott insulating materials and further investigations of models where the kinetic energy is instead reduced by frustration of isotropic couplings^{19,20} are clearly called for if connection to experiments is ever to be made.

In this context, the recent report of a spin-SS phase in a spin-half frustrated DAF by Chen *et al.*,²⁰ who have relied on a novel tensor-product algorithm, is an important result. However, in view of the first-order transitions observed in the related case of the Shastry-Sutherland model, a systematic investigation of the possibility of phase separation (PS) is still required.

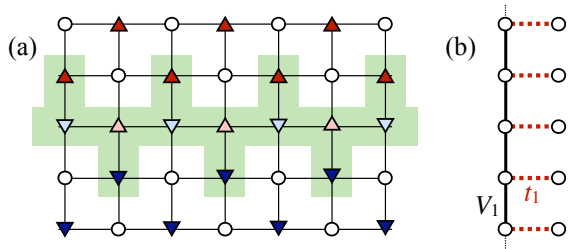


FIG. 1: (Color online) (a) A DW between mismatching domains in a CBS doped with holes is highlighted: open circles represent hard-core bosons (triplets) and holes/singlets in the upper (lower) domain are indicated by upward (downward) triangles; *doped* holes are shown as light-filled upward or downward triangles. (b) A simplified model for the DW, valid for $V_1/t_1 \gg 1$, is defined on a “comb” geometry: holes hop (with amplitude t_1) through the links indicated by dashed lines and repel, with strength V_1 , one another along the vertical nearest-neighbor links indicated by solid lines.

In this paper, we investigate the interplay between SS order and PS in the frustrated DAF analyzed in Ref. 20. We begin by estimating the energetic gains behind PS and supersolidity for hard-core bosons on the square lattice by relying on strong coupling arguments, and introduce an indicator of the instability toward PS. We then proceed to the analysis of effective bosonic models obtained from the application of the Contractor Renormalization (CORE) algorithm²¹ to the DAF investigated in Ref. 20. The so-obtained effective Hamiltonians are studied by performing self-consistent cluster mean-field theory (SCMFT) calculations and tendency toward PS is gauged through means of the aforementioned indicator.

II. PHASE SEPARATION VERSUS SUPERSOLIDITY FOR LATTICE BOSONS

In this section, we analyze the interplay between PS and supersolidity in models of hard-core bosons on the square lattice, onto which the low-energy physics of the spin model considered in the remainder of this paper can be mapped.

A. Instability to Domain Wall Formation

We start by considering the simplest model of hard-core bosons on the square lattice, the so-called $t - V$ model:

$$\mathcal{H}_{t-V} = -t_1 \sum_{\langle i,j \rangle} (b_i^\dagger b_j + \text{H.c.}) + V_1 \sum_{\langle i,j \rangle} n_i n_j - \mu \sum_i n_i. \quad (1)$$

$n_i = b_i^\dagger b_i$ is the occupation number operator for *holes*²² at site i (a hard-core constraint is imposed), whose density is controlled by the chemical potential μ . Here, only

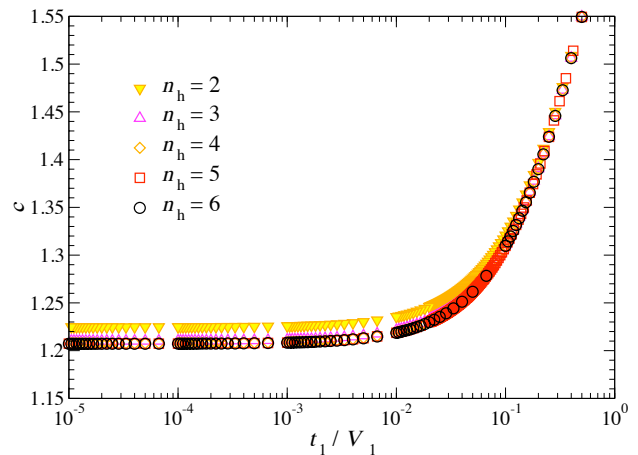


FIG. 2: (Color online) $c = -E_{\text{DW}}/n_h t_1$ obtained from EDs on the geometry depicted in Fig. 1(b), for clusters comprising from $N = 8$ ($n_h = 2$) to $N = 24$ ($n_h = 6$) sites.

nearest-neighbor (NN) hopping (t_1) and interaction (V_1) terms are considered but, as will be discussed later, the effective model derived for the spin model Eq. (3) further comprises longer-ranged and/or multi-body couplings.

The model Eq. (1) had been for many years conjectured to support SS phases (see Refs. 23,24 and references therein), but a more systematic numerical analysis²⁴ later disproved earlier evidences in favor of this scenario and showed that, instead, PS prevents the occurrence of supersolidity. An intuitive explanation for such behavior was put forward in Ref. 25 by relying on strong coupling arguments. Following this analysis,²⁵ holes [or also particles in the case of Eq. (1);²² however, the effective models to be analyzed later lack particle-hole symmetry] doped into the CBS ground-state of Eq. (1) for $V_1/t_1 \gg 1$ at half-filling would delocalize with an effective hopping amplitude proportional to t_1^2/V_1 and eventually condense, giving origin to SS order. However, this last conclusion is flawed in that it ignores the possibility of PS. Indeed, in the strongly interacting regime domain wall [DW, depicted as the shaded region in Fig. 1(a)] formation is energetically favored for the model Eq. (1): the energetic gain per *doped* hole (we denote the number of *doped* holes by n_h) is *linear* in t_1 under these circumstances, $E_{\text{DW}}/n_h \sim -ct_1$ with $c \in [1, 2]$.²⁵

Since one of our primary goals in the present work is to investigate the interplay between PS and supersolidity, so to be able to decide which among the two possibilities take place for the spin model herein analyzed [Eq. (3)], we would like to obtain a more accurate estimate for $E_{\text{DW}}/n_h t_1$; in other words, we would like to pinpoint the actual values assumed by $c \in [1, 2]$. In achieving this goal we completely ignore fluctuations in CBS-ordered regions away from DWs, a supposedly good approximation for $V_1/t_1 \gg 1$, and consider a simplified $t - V$ -like model at half-filling (quarter-filling for *doped* holes) defined on the “comb” geometry depicted in Fig. 1(b). In

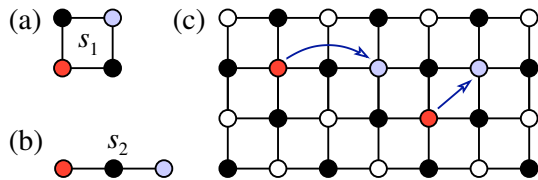


FIG. 3: (Color online) (a-b) Correlated hoppings behind the “leapfrog mechanism” for supersolidity [holes hop in between red and light-blue sites *only* if the dark circles are occupied by holes — in (a), at least one of the sites must be occupied; if both are, the amplitude is $2s_1$], that allow extra holes to delocalize in a CBS background by leapfrogging on the other sublattice (c). Adapted from Ref. 18.

such a simplified model hopping processes with amplitude t_1 only take place in between NN sites linked by the comb’s “teeth” and interaction V_1 is only active for holes sitting on NN sites along the “backbone” [see Fig. 1(b)].

In Fig. 2 we plot results for $c = -E_{\text{DW}}/n_h t_1$, as a function of t_1/V_1 , obtained from exact diagonalizations (EDs) of the just discussed simplified model on the comb geometry depicted in Fig. 1(b), for clusters comprising up to $N = 24$ sites (thus, up to $n_h = 6$ doped holes). We first notice that $c \approx 1.2$ in the limit of large V_1/t_1 . On the other hand, since fluctuations away from the DW are ignored in our analysis, we expect our ED results to *underestimate* c for small values of V_1/t_1 . Nonetheless, we keep this limitation in mind and throughout the remainder of this paper rely on ED results in estimating the DW energy even in the weakly interacting regime $V_1/t_1 \sim 2$. In doing so, we take advantage of the very small finite size effects in the data shown in Fig. 2 and obtain c from EDs on finite clusters.

B. Leapfrog Mechanism for Supersolidity

In a previous work,¹⁸ we have shown that the instability toward PS is suppressed in models of hard-core bosons on the square lattice that include, in addition to the terms comprised in the $t - V$ model [Eq. (1)], the correlated hopping processes with amplitudes s_1 and s_2 depicted in Fig. 3. Indeed, such correlated hopping terms have been shown^{18,26} to favor supersolidity by allowing doped holes to delocalize on top of a CBS by “leapfrogging” on the other sub-lattice. We wish now to devise a criterion for determining how large should the amplitudes s_1 and s_2 be so to inhibit DW formation and thus stabilize a SS. In doing so, we once more rely on strong coupling arguments, and estimate the energetic gain associated to the leapfrog processes represented in Fig. 3 as

$$E_{\text{SS}}/n_h = -4(2|s_1| + |s_2|) . \quad (2)$$

That is, E_{SS}/n_h is simply the ground-state energy of a single hole doped into a “frozen” CBS, an approximation

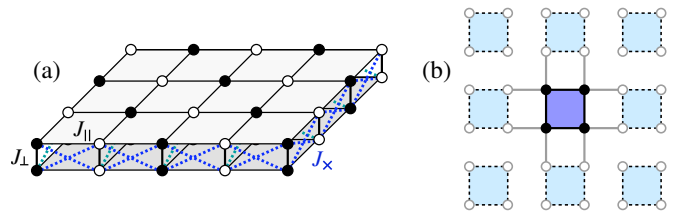


FIG. 4: (Color online) (a) Antiferromagnetic bilayer investigated in this paper [Eq. (3)], with couplings: J_\perp (thick vertical lines), J_\parallel (thinner in-layer lines) and J_x (dashed lines). A magnetic field h promotes singlets (vertical pairs of filled circles) to triplets (pairs of open circles); a CBS configuration at half-filling is depicted. (b) $N = 2 \times 2$ cluster for SCMFT: interactions (thick black lines) involving only in-cluster sites (dark-filled circles) are treated exactly while couplings to the environment (grey lines) in a MF way. Although only NN bonds are depicted, the effective model from CORE also includes longer-ranged terms.

expected to hold for $V_1/t_1 \gg 1$, hopping via the processes with amplitude s_1 and s_2 [Fig. 3(a-b)]. As it happens for our estimate $E_{\text{DW}}/n_h = -ct_1$ obtained in Sec. II A, we expect E_{SS}/n_h as given by Eq. (2) to underestimate the actual energetic gain associated to the leapfrog processes.

We combine the just presented analysis and the one discussed in Sec. II A concerning DW formation and introduce an indicator for analyzing the interplay between supersolidity and PS: the difference between E_{SS}/n_h [Eq. (2)] and $E_{\text{DW}}/n_h = -ct_1$ (obtained from EDs by using V_1/t_1 as input; see Secs. II A), our estimates for the energetic gains respectively associated to each of these possibilities. Since both estimates are obtained from strong coupling analysis, the indicator $(E_{\text{SS}} - E_{\text{DW}})/n_h$ can only be expected to be accurate in the limit of $V_1/t_1 \gg 1$. However, we keep this limitation in mind and in the analysis to be performed in Sec. III, we rely on $(E_{\text{SS}} - E_{\text{DW}})/n_h$ as an indicator even for couplings $V_1/t_1 \sim 2$.

III. FRUSTRATED SPIN MODEL

A. Model and Effective Hamiltonian

In most of the lattice models that have, so far, been shown to display SS properties the effective repulsion (necessary to destabilize the uniform superfluid and induce a SS state) stems from the presence of nearest-neighbor repulsive terms in XXZ Hamiltonians.^{17,18,27} While these anisotropic models are interesting from a theoretical perspective, their strong anisotropic character renders them unrealistic for antiferromagnetic Mott insulators. More promising in this sense is the frustrated spin-half Hamiltonian analyzed in Ref. 20, defined on a

bilayer geometry [Fig. 4(a)]

$$\mathcal{H} = \sum_{\langle i,j \rangle} \left[\sum_{\alpha=1,2} J_{\parallel} \mathbf{S}_{i,\alpha} \cdot \mathbf{S}_{j,\alpha} + J_{\times} (\mathbf{S}_{i,1} \cdot \mathbf{S}_{j,2} + \mathbf{S}_{i,2} \cdot \mathbf{S}_{j,1}) \right] + \sum_i \left[J_{\perp} \mathbf{S}_{i,1} \cdot \mathbf{S}_{i,2} - h \sum_{\alpha=1,2} S_{i,\alpha}^z \right]. \quad (3)$$

$\langle i,j \rangle$ denotes NN sites in each square layer α of the frustrated bilayer depicted in Fig. 4(a). J_{\perp} couples spins in different layers to build the basic dimers of the model (we set $J_{\perp} = 1$). The applied magnetic field h acts as a chemical potential, promoting spin-dimers from a singlet (hole) to a triplet (triplon) state. Effective interactions appear as the result of in-layer J_{\parallel} and frustrating J_{\times} antiferromagnetic couplings. We remark that the lattice depicted in Fig. 4(a) remains invariant if every other spin-dimer is rotated by π and thus Eq. (3) is invariant under the transformation $J_{\parallel} \leftrightarrow J_{\times}$, with the consequence that the phase diagram is symmetric about the line $J_{\parallel} = J_{\times}$.

In studying the model of Eq. (3), we adopt an approach similar to the one employed in our previous work Ref. 18, where a related unfrustrated model was investigated and to which the reader is referred for details,²² and derive an effective bosonic model by relying on the CORE algorithm.²¹ We consider spin-dimers connected by J_{\perp} as elementary blocks and select the singlet $|s\rangle = \frac{1}{\sqrt{2}}[|\uparrow\downarrow\rangle - |\downarrow\uparrow\rangle]$ and the $S^z = +1$ triplet $|t^+\rangle = |\uparrow\uparrow\rangle$ as the block states in the CORE expansion: for all parameters in Eq. (3) considered in the present work, $J_{\parallel}, J_{\times} \in [0, 0.5]$, this choice is justified by the large reduced density-matrix weights associated to such block states and by the rapid convergence of effective couplings for increasing range in the expansion.²⁸ Effective couplings are derived by diagonalizing clusters of coupled dimers and by projecting a matching number of low-lying cluster eigenstates onto the basis formed by tensor products of the retained block states, $|s\rangle$ and $|t^+\rangle$.²⁹ The effective bosonic Hamiltonian thus obtained is essentially identical to the one derived for the anisotropic model studied in Ref. 18, *only* the magnitudes for each coupling being different. Similarly, the effective model obtained here is *not* invariant under particle-hole transformation and, in particular, amplitudes for “leapfrog processes” are non-zero only when *holes* are involved. From this last observation we expect that only hole-doped SS phases can be stabilized in the spin-dimer model Eq. (3) and conclude that the effective Hamiltonian is more conveniently expressed in terms of hole operators ($n_i = b_i^\dagger b_i$ is the occupation number for holes at the dimer-lattice site \mathbf{r}_i). We therefore adopt the same notation as in our previous work,^{18,22} to which the reader is referred for a complete list of single- and multi-hole interactions and hopping processes [see Eqs. (8, B1-B5) in Ref. 18]. We also remark that the effective Hamiltonian preserves the symmetry of the original model Eq. (3) and remains invariant under $J_{\parallel} \leftrightarrow J_{\times}$.

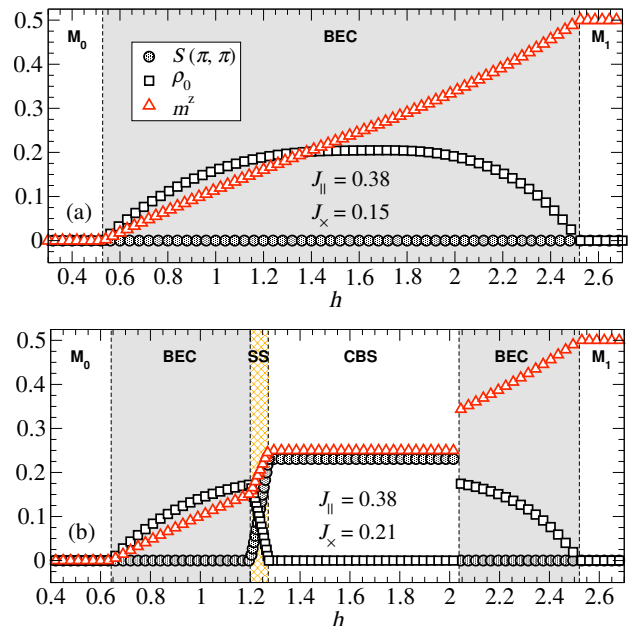


FIG. 5: (Color online) SCMFT results for the condensate density ρ_0 [squares, Eq. (4)], CBS structure factor $S(\pi, \pi)$ [circles, Eq. (5)] and magnetization density [triangles, Eq. (6)] for the effective CORE Hamiltonian for Eq. (3) with couplings $(J_{\parallel}, J_{\times})$ considered in Ref. 20: (a) (0.38, 0.15) and (b) (0.38, 0.21). Successive phases for increasing magnetic field h are labeled as: spin-gapped (M_0), condensate (BEC), supersolid (SS), checkerboard solid (CBS) and fully polarized (M_1).

B. Mean-Field Approach

Effective Hamiltonians resulting from CORE are often complex and different strategies may be pursued in trying to extract physically sound results from them. One possibility is the mean-field (MF) theory of Ref. 18, which reproduces semi-quantitatively the results of quantum Monte Carlo (QMC) simulations¹⁷ for the anisotropic spin-dimer model considered therein. However, MF calculations are known to overestimate the extent of SS phases and it would be desirable to include, at least partially, effects due to quantum fluctuations. From this perspective, the SCMFT³⁰ that partially takes local quantum fluctuations into account and has been recently applied to the $t-V$ model for hard-core bosons on the triangular lattice³¹ seems particularly well suited for our purposes. Indeed, the extent of the SS phase in the ground-state phase diagram obtained by applying SCMFT to the $t-V$ model on the triangular lattice³¹ compares considerably better with results from QMC simulations²⁷ than what is found from a more conventional MF approach.³²

SCMFT is applied by diagonalizing the effective CORE Hamiltonian on the $N = 2 \times 2$ cluster depicted in Fig. 4(b). In setting the cluster’s Hamiltonian, in-cluster interactions are treated *exactly* while couplings to the environment in a self-consistent way: for instance, a given

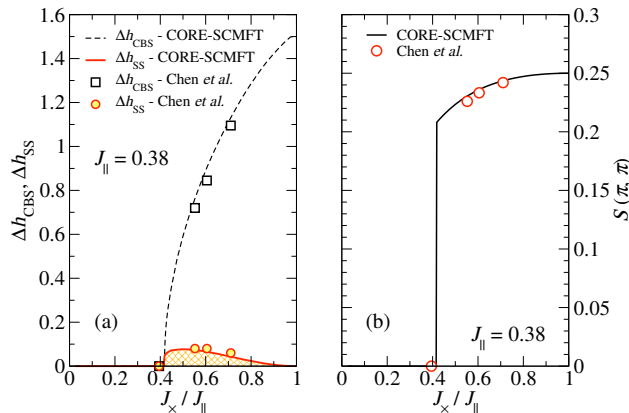


FIG. 6: (Color online) $J_{\parallel} = 0.38$. (a) Extent of CBS (Δh_{CBS}) and SS (Δh_{SS}) phases [maximum minus minimum value of the field h leading to the corresponding phase for given parameters (J, J_{\times})]. (b) Value of the structure factor [Eq. (5)] at the CBS plateau. In (a) and (b), symbols indicate results by Chen *et al.*²⁰ and lines the here obtained results.

interaction connecting sites \mathbf{r}_i and \mathbf{r}_j contributes a term proportional to $n_i n_j$ for each in-cluster bond [thick black lines in Fig. 4(b)] and with mean-field terms of the form $[n_i \langle n_j \rangle + \langle n_i \rangle n_j]$ for “bonds” connecting the cluster to its environment [grey lines in Fig. 4(b)]. At each step, the ground-state for the cluster Hamiltonian is calculated and expectation values $\langle n_i \rangle$, $\langle b_i \rangle$ at every site \mathbf{r}_i computed; these are then used in setting the mean fields for the next iteration, until convergence is achieved (see Ref. 31 for details). In this way, we compute the condensate density at the point $\mathbf{k}_0 = (\pi, \pi)$

$$\rho_0 = \left| \frac{1}{N} \sum_j e^{i\mathbf{k}_0 \cdot \mathbf{r}_j} \langle b_j \rangle \right|^2, \quad (4)$$

the CBS structure factor (normalized per site)

$$S(\pi, \pi) = \frac{1}{N^2} \sum_{j,l} e^{i\mathbf{k}_0 \cdot (\mathbf{r}_j - \mathbf{r}_l)} \langle n_j n_l \rangle, \quad (5)$$

and the magnetization along the field direction

$$m^z = \frac{1}{2N} \sum_i \langle (1 - n_i) \rangle. \quad (6)$$

In Fig. 5 we plot these quantities as a function of the magnetic field h for couplings considered in Ref. 20, $(J_{\parallel}, J_{\times}) = (0.38, 0.15)$ and $(0.38, 0.21)$. We first notice that the overall agreement between our results and the data presented in Ref. 20 is remarkably good.³³ For the least frustrated case of $(J_{\parallel}, J_{\times}) = (0.38, 0.15)$ [Fig. 5(a)], the system first undergoes a quantum transition from a spin-gapped (equivalent to a trivial bosonic Mott insulator with zero-filling for triplons, M_0 in Fig. 5) to a BEC phase at the lower critical field h_{c1} , and then from

the BEC to a fully polarized phase (trivial Mott insulator with unitary triplon filling, M_1) at the upper critical field h_{c2} . More interestingly, additional CBS and SS phases are stabilized for the more frustrated case of $(J_{\parallel}, J_{\times}) = (0.38, 0.21)$ [Fig. 5(b)]. The existence of a SS phase at the low-field boundary of the CBS plateau, with finite values for both ρ_0 and $S(\pi, \pi)$ is at least partially due to the presence of correlated hoppings for *holes* in the effective CORE Hamiltonian. Indeed, no SS phase is observed for an “effective model” obtained by setting $s_1 = s_2 = 0$ [Fig. 3(a-b)] while keeping all the other effective couplings unchanged. This situation is to be contrasted with the first-order transition from CBS to BEC at higher fields, explained by the *vanishing* amplitudes for correlated hoppings for *triplons* for all values $J_{\parallel}, J_{\times} \in [0, 0.5]$.

We proceed by varying the frustrating coupling J_{\times} while fixing $J_{\parallel} = 0.38$. In Fig. 6(a) we plot the extent of the SS, CBS phase, respectively $\Delta h_{\text{SS}, \text{CBS}} = h_{\text{SS}, \text{CBS}}^{\text{max}} - h_{\text{SS}, \text{CBS}}^{\text{min}}$ [$h_{\text{SS}, \text{CBS}}^{\text{max}}$ ($h_{\text{SS}, \text{CBS}}^{\text{min}}$) denotes the upper (lower) boundary of the SS, CBS phase] as a function of J_{\times}/J_{\parallel} . In order to further gauge the accuracy of the here employed CORE-SCMFT approach in Fig. 6(a) our results for Δh_{SS} and Δh_{CBS} are compared against those from Ref. 20 and in Fig. 6(b) we plot both our results and those from Ref. 20 for the structure factor $S(\pi, \pi)$ at the CBS plateau. Excellent agreement is found in both cases and we further remark that our results for $S(\pi, \pi)$ in the CBS phase in Fig. 6(b) confirm that quantum fluctuations are indeed partially taken into account by SCMFT: in contrast to what happens with the semi-classical MF approach employed in Ref. 18, here the value of $S(\pi, \pi)$ at the plateau is somewhat reduced from its classical value $S_{\text{classical}}(\pi, \pi) = 1/4$.

At this point, and despite of its aforementioned attractive features, it is important to have in mind an important limitation of the here employed SCMFT procedure: since calculations rely on diagonalizations of a 2×2 cluster [Fig. 4(b)], only *homogeneous* solutions, displaying order consistent with at most quadrupling of the unit cell, are obtainable. This excludes *inhomogeneous* solutions such as those associated with the presence of DWs [Fig. 1(a)] and has the consequence that our combined CORE-SCMFT approach is insensitive to the occurrence of PS. In what follows, we rely on the strong coupling analysis presented in Sec. II and analyze the interplay between PS and spin-SS order in the phase diagram of the model Eq. (3).

C. Phase Diagram and Phase Separation

We now turn our attention to the obtention of a global $J_{\parallel} - J_{\times}$ phase diagram that may guide the experimental search for realizations of spin-supersolidity and therefore extend our analysis by varying J_{\parallel} in Eq. (3). In Fig. 7(a) we plot Δh_{SS} as a function of $J_{\parallel}, J_{\times} \in [0, 0.5]$, obtained from the combined CORE-SCMFT procedure. These

results suggest that, far from being a rare occurrence, spin-supersolidity is widespread throughout the parameter space and can extend over fairly wider ranges of h than it is observed for the value $J_{\parallel} = 0.38$ [couplings considered in Ref. 20 are highlighted in Fig. 7(a)]. However, under the light of our discussion in Sec. II concerning PS in systems of hard-core bosons on a lattice, some caution is required in drawing conclusions from the results shown in Fig. 7(a).

Following the discussion in Sec. II, we evaluate $(E_{SS} - E_{DW})/n_h t_1$, our indicator for analyzing the interplay between PS and supersolidity for hard-core bosons on the square lattice, as a function of $J_{\parallel}, J_{\times} \in [0, 0.5]$ for Eq. (3). E_{SS}/n_h , our strong coupling estimate for the energetic gain associated to occurrence of SS order, is readily obtained by plugging the amplitudes for the leapfrog processes s_1 and s_2 [Fig. 3(a-b)] obtained from CORE into Eq. (2). On the other hand, the estimate E_{DW}/n_h for the energy associated to PS is obtained from numerical EDs for the simplified model for DWs defined on the ‘‘comb geometry’’ discussed in Sec. II A by using the effective ratio V_1/t_1 , as obtained from the CORE expansion for each set $J_{\parallel}, J_{\times}$ in Eq. (3), as an input. EDs are performed on a small cluster comprising $N = 16$ sites ($n_h = 4$ doped holes): as mentioned in Sec. II A, this is justified by the absence of sizable finite size effects for the data displayed in Fig. 2.

We plot $(E_{SS} - E_{DW})/n_h t_1$ as a function of $J_{\parallel}, J_{\times} \in [0, 0.5]$ in Fig. 7(b) and assume that two conditions must be simultaneously fulfilled for SS phases to exist for the model Eq. (3): (i) a SS must be observed within CORE-SCMFT and (ii) $(E_{SS} - E_{DW})/n_h t_1 < 0$. Values of $J_{\parallel}, J_{\times}$ leading to $(E_{SS} - E_{DW})/n_h t_1 = 0$, the threshold value for a SS phase to appear, are indicated by the thick continuous curve in Fig. 7. We notice that not all values of $J_{\parallel}, J_{\times}$ yielding a spin-SS phase within our CORE-SCMFT approach fulfill $(E_{SS} - E_{DW})/n_h t_1 < 0$ and expect PS to take place under these circumstances instead. Despite of the fact that the condition $(E_{SS} - E_{DW})/n_h t_1 < 0$ considerably shrinks the size of the region expected to support SS phases from a pure CORE-SCMFT analysis, supersolidity is still observed for a wide range of couplings in Eq. (3) [Fig. 7(a)], possibly realizable in real magnets.

Intriguingly, we notice that the parameters (circles in Fig. 7) for which a spin-SS phase has been detected by Chen *et al.*,²⁰ and also by the pure CORE-SCMFT analysis devised here (Figs. 5 and 6), fail to satisfy $(E_{SS} - E_{DW})/n_h t_1 < 0$ [Fig. 7(b)]. Although we cannot exclude the possibility that our criterion, that rigorously applies only in the limit $V_1/t_1 \gg 1$, is too stringent for the frustrated model Eq. (3), we remark that a SS phase is obtained within our CORE-SCMFT approach³⁴ and in Ref. 20 even for couplings $J_{\parallel} \sim J_{\times}$, where our strong coupling arguments become accurate [the ratio V_1/t_1 diverges toward the line $J_{\parallel} = J_{\times}$; see Fig. 7(b), where contour levels for V_1/t_1 are plotted as thin continuous lines]. This inconsistency suggests that both CORE-SCMFT and the novel algorithm employed in Ref. 20 are insensi-

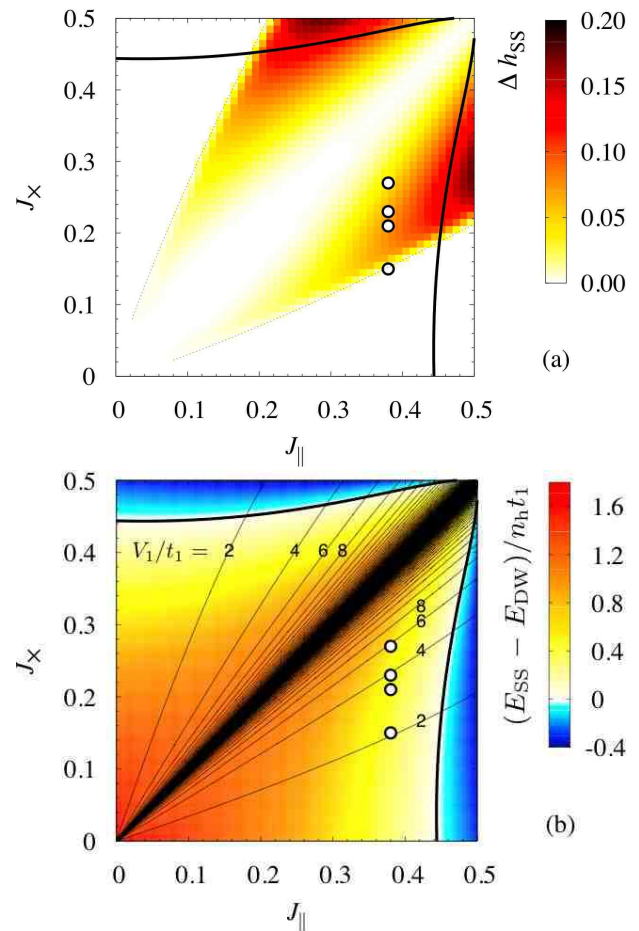


FIG. 7: (Color online) (a) SCMFT results for the extent of the SS phase Δh_{SS} (see main text) for the frustrated DAF Eq. (3). The symmetry $J_{\parallel} \leftrightarrow J_{\times}$ has been explored in obtaining the data. Regions where supersolidity [PS] is expected, where $(E_{SS} - E_{DW})/n_h t_1 < 0$ [$(E_{SS} - E_{DW})/n_h t_1 > 0$] are marked by the label SS [PS]. Dashed lines indicate threshold values for a CBS/SS to appear at the mean-field level. (b) $(E_{SS} - E_{DW})/n_h t_1$, as obtained from EDs on an $N = 16$ ($n_h = 4$ doped holes) site cluster with the comb geometry depicted in Fig. 1(b), for the model Eq. (3). Contour levels for V_1/t_1 (obtained from the CORE expansion) are indicated by thin lines and the values $V_1/t_1 = 2, 4, 6$ and 8 are highlighted. In both panels, circles indicate couplings investigated by Chen *et al.*²⁰ and the thick line couplings yielding the threshold value $(E_{SS} - E_{DW})/n_h t_1 = 0$.

tive to the instability toward PS in systems of hard-core bosons on the square lattice and that the obtention of SS phase for $(E_{SS} - E_{DW})/n_h t_1 > 0$ is *spurious*.³⁴ It would therefore be important to further test the ability of the algorithm employed in Ref. 20 to detect PS in bosonic lattice models by, for instance, checking how it compares to QMC for the unfrustrated model studied in Refs. 17,18 regarding this issue.

IV. SUMMARY

Summarizing, we have studied a spin-half frustrated bilayer model by combining CORE and SCMFT. Our results reveal the presence of a spin-SS phase under applied magnetic field, which appears at the edge of a half-saturated magnetization plateau and is stabilized by a “leapfrog mechanism”.¹⁸ We address the interplay between supersolidity and instability toward PS, that precludes the emergence of spin-SS phases, by devising a quantitative criterion based on strong coupling arguments. This criterion is generically applicable to systems of hard-core bosons on the square lattice, and it would be interesting to further assess its validity by investigating models where the interplay between PS and SS can be independently analyzed. By relying on this

criterion, we obtain a global phase diagram for the frustrated spin-dimer antiferromagnet considered herein, and show that a spin-SS phase is stable against PS for couplings realizable in real magnets. We expect that our results may guide the experimental search for systems exhibiting spin-supersolidity.

Acknowledgments

We acknowledge fruitful discussions with C. D. Batista and M. Troyer, as well as funding from the French ANR program ANR-08-JCJC-0056-01, from ARC (Australia), from the SNF and from MaNEP (Switzerland). NL acknowledges LPT Toulouse for hospitality.

-
- ¹ T. Giamarchi, C. Rüegg, and O. Tchernyshyov, *Nat. Phys.* **4**, 198 (2008).
- ² F. Mila, *Eur. Phys. J. B* **6**, 201 (1998).
- ³ K. Totsuka, *Phys. Rev. B* **57**, 3454 (1998); T. Giamarchi and A. M. Tsvelik, *Phys. Rev. B* **59**, 11398 (1999).
- ⁴ S. E. Sebastian, N. Harrison, C. D. Batista, L. Balicas, M. Jaime, P. A. Sharma, N. Kawashima, and I. R. Fisher, *Nature* **441**, 617 (2006).
- ⁵ C. Rüegg, D. F. McMorrow, B. Normand, H. M. Rønnow, S. E. Sebastian, I. R. Fisher, C. D. Batista, S. N. Gvasaliya, C. Niedermayer, and J. Stahn, *Phys. Rev. Lett.* **98**, 017202 (2007).
- ⁶ S. Krämer, R. Stern, M. Horvatić, C. Berthier, T. Kimura, and I. R. Fisher, *Phys. Rev. B* **76**, 100406 (2007).
- ⁷ N. Laflorencie and F. Mila, *Phys. Rev. Lett.* **102**, 060602 (2009).
- ⁸ M. Takigawa and F. Mila, in *Introduction to Frustrated Magnetism*, edited by C. Lacroix, P. Mendels, and F. Mila (Springer - Berlin, 2011).
- ⁹ H. Kageyama, K. Yoshimura, R. Stern, N. V. Mushnikov, K. Onizuka, M. Kato, K. Kosuge, C. P. Slichter, T. Goto, and Y. Ueda, *Phys. Rev. Lett.* **82**, 3168 (1999).
- ¹⁰ K. Kodama, M. Takigawa, M. Horvatić, C. Berthier, H. Kageyama, Y. Ueda, S. Miyahara, F. Becca, and F. Mila, *Science* **298**, 395 (2002).
- ¹¹ J. Dorier, K. P. Schmidt, and F. Mila, *Phys. Rev. Lett.* **101**, 250402 (2008); A. Abendschein and S. Capponi, *Phys. Rev. Lett.* **101**, 227201 (2008).
- ¹² A. F. Andreev and I. M. Lifshitz, *Sov. Phys. JETP* **29**, 1107 (1969).
- ¹³ E. Kim and M. H. W. Chan, *Nature* **427**, 225 (2004); E. Kim and M. H. W. Chan, *Science* **305**, 1941 (2004).
- ¹⁴ S. Balibar, *Nature* **464**, 176 (2010).
- ¹⁵ T. Senthil, A. Vishwanath, L. Balents, S. Sachdev, and M. P. A. Fisher, *Science* **303**, 1490 (2004).
- ¹⁶ T. Momoi and K. Totsuka, *Phys. Rev. B* **62**, 15067 (2000).
- ¹⁷ K.-K. Ng and T. K. Lee, *Phys. Rev. Lett.* **97**, 127204 (2006); N. Laflorencie and F. Mila, *Phys. Rev. Lett.* **99**, 027202 (2007).
- ¹⁸ J.-D. Picon, A. F. Albuquerque, K. P. Schmidt, N. Laflorencie, M. Troyer, and F. Mila, *Phys. Rev. B* **78**, 184418 (2008).
- ¹⁹ P. Sengupta and C. D. Batista, *Phys. Rev. Lett.* **98**, 227201 (2007).
- ²⁰ P. Chen, C.-Y. Lai, and M.-F. Yang, *Phys. Rev. B* **81**, 020409 (2010).
- ²¹ C. J. Morningstar and M. Weinstein, *Phys. Rev. Lett.* **73**, 1873 (1994); C. J. Morningstar and M. Weinstein, *Phys. Rev. D* **54**, 4131 (1996).
- ²² The model Eq. (1) displays particle-hole symmetry, unlike the effective model for the spin model Eq. (3). Throughout this paper, we follow a notation similar to the one adopted in our previous work Ref. 18, but omit the tildes appearing therein. That is, for instance, amplitudes for the correlated processes for *holes* depicted in Fig. 3 are here written as $s_{1,2}$ while in Ref. 18 those were denoted by $\tilde{s}_{1,2}$.
- ²³ R. T. Scalettar, G. G. Batrouni, A. P. Kampf, and G. T. Zimanyi, *Phys. Rev. B* **51**, 8467 (1995);
- ²⁴ G. G. Batrouni and R. T. Scalettar, *Phys. Rev. Lett.* **84**, 1599 (2000).
- ²⁵ P. Sengupta, L. P. Pryadko, F. Alet, M. Troyer, and G. Schmid, *Phys. Rev. Lett.* **94**, 207202 (2005).
- ²⁶ K. P. Schmidt, J. Dorier, A. M. Läuchli, and F. Mila, *Phys. Rev. Lett.* **100**, 090401 (2008).
- ²⁷ S. Wessel and M. Troyer, *Phys. Rev. Lett.* **95**, 127205 (2005); R. G. Melko, A. Paramekanti, A. A. Burkov, A. Vishwanath, D. N. Sheng, and L. Balents, *Phys. Rev. Lett.* **95**, 127207 (2005); D. Heidarian and K. Damle, *Phys. Rev. Lett.* **95**, 127206 (2005); M. Boninsegni and N. Prokof'ev *Phys. Rev. Lett.* **95**, 237204 (2005).
- ²⁸ A. Abendschein and S. Capponi, *Phys. Rev. B* **76**, 064413 (2007).
- ²⁹ In this way, and by imposing that each cluster's low-energy spectrum is exactly reproduced, effective couplings of up to range-2 (see Fig. 5 in Ref. 18) are computed.
- ³⁰ E. Zhao and A. Paramekanti, *Phys. Rev. B* **76**, 195101 (2007).
- ³¹ S. R. Hassan, L. de Medici, and A.-M. S. Tremblay, *Phys. Rev. B* **76**, 144420 (2007).
- ³² G. Murthy, D. Arovas, and A. Auerbach, *Phys. Rev. B* **55**, 3104 (1997).
- ³³ Similarly good agreement is found for the other couplings considered in Ref. 20, $(J, J_{\times}) = (0.38, 0.23)$ and $(0.38, 0.27)$.

³⁴ A SS phase is obtained from the CORE-SCMFT procedure for *arbitrarily small* amplitudes for the leapfrog processes depicted in Fig. 3(a-b). First order transitions are only observed when correlated processes *vanish*, as it is the case

for the higher-field transition out from the CBS plateau in Fig. 5(b) (correlated hoppings for triplons vanish for all $J, J_{\times} \in [0, 0.5]$).